ISSN 2411-3336; e-ISSN 2541-9404

JOURNAL OF MINING INSTITUTE

Zapiski Gornogo instituta

Journal homepage: pmi.spmi.ru

*Research article*

# Trace element composition of silicate minerals from Kunashak Meteorite (L6)

**Kristina G. Sukhanova✉, Olga L. Galankina**

*Institute of Precambrian Geology and Geochronology RAS, Saint Petersburg, Russia*

***How to cite this article*:** Sukhanova K.G, Galankina O.L. Trace element composition of silicate minerals from Kunashak Meteorite (L6). Journal of Mining Institute. 2024. Vol. 270, p. 877-892.

***Abstract***

Major (EPMA) and trace (SIMS) element geochemistry in the silicate minerals (olivine, pyroxene and plagioclase) of Kunashak equilibrated ordinary chondrite (L6) is described. No variations in the major element concentrations of the silicate minerals have been found, which is characteristic of equilibrated chondrites of petrological type VI. Low-Ca pyroxene and plagioclase from the radiated olivine-pyroxene chondrule of Kunashak Meteorite contain an abundance of trace elements (Yb, Cr, Nb and Ti – pyroxene; Sr, Y, Ti and Zr – plagioclase), which is not characteristic of minerals from the porphyritic olivine and olivine-pyroxene chondrules of the meteorite. The porphyritic olivine-pyroxene chondrule of the Kunashak Meteorite has high trace element concentrations in olivine, in particular, the highest Yb concentration (0.12 ppm on the average) relative to porphyritic and radiated olivine-pyroxene chondrules (0.02 ppm). High trace element concentrations indicate rapid crystallization of a radiated chondrule in a nebula and show no traces of trace element homogenization upon thermal metamorphism. The trace element composition of silicate minerals from Kunashak Meteorite has retained the individual melting pattern of the chondrules and remained unaffected by thermal metamorphism on the parent bodies of the chondrules. Similar results, obtained in the study of Bushkhov Meteorite (L6), indicate that trace elements in olivine and low-Ca pyroxene are resistant to thermal metamorphism. The persistence of the individual pattern of the chondrules enables us to use equilibrated ordinary chondrites for the study of processes at early stages in the formation of the Solar System and to better understand chondrule and planet formation mechanisms.

***Keywords***

Ordinary chondrites; trace elements; olivine; pyroxene; plagioclase; ion probe

***Funding***

The study was carried out within the framework of the research topic of the IPGG RAS (N FMUW-2022-0005).

***Received: 08.11.2023*** ***Accepted: 02.05.2024*** ***Online: 26.07.2024*** ***Published: 25.12.2024***

## Introduction.

Kunashak stone meteorite rain fell on June 11th, 1949, at 8:14 a.m. local time, in the Kunashak District, Chelyabinsk Region. The falling of the bolide was accompanied by bright light in the sky, 350 km from the falling site. The workers of the Chelyabinsk Teachers' Training Institute, the Mining and Geological Institute at the Uralian Branch of the USSR Academy of Sciences and representatives of the Committee for Meteorites, USSR Academy of Sciences, together with local residents, collected and described 13 fragments of the meteorite totaling about 200 kg in weight and calculated the falling trajectory of the meteorite and the dispersion ellipse of the fragments [1].

It was shown in early descriptions that the meteorite is divided by a sharp boundary into black and light-grey sectors, that it has neither melting crust nor regmaglypts and that it has abundant solidified jets and drops of plessite and silicates [1]. In 1951, local residents found two 250 and 700 g fragments [2]. Another fragment weighing 2.5 kg was found in the summer of 2014 [3]. In 1960, the frontal portion of the dispersion ellipse of Kunashak Rain was shown to contain meteorite dust particles [4]. The details of the falling [5] and the meteorite's orbit parameters [6] were determined later. The meteorite was studied thoroughly by Russian and foreign researchers and was used for comparison of methods employed for analyzing the composition of small bodies in the Solar System [7].

Kunashak Meteorite is of a group of olivine-hypersthene low-iron equilibrated ordinary chondrites (L6). Equilibrated ordinary chondrites (EOC) are the most common group of meteorites known



This is an open access article under the CC BY 4.0 license

on earth, making up 90 % of the entire meteoritic matter. Chondrites consist of silicate spherules (chondrules), less than 1 mm in size, composed of olivine, low-Ca pyroxene and mesostasis. The chondrules, occurring as drops of melt solidified at zero gravity in a nebula, are the oldest objects in the Solar system [8, 9]. Chondrules vary in structure and are divided into two groups: porphyritic and nonporphyritic (radiated, barred, granular, cryptocrystalline, etc.). The diversity of the structural types of chondrules indicates variations in their conditions of formation in a nebula.

Experiments on the reproduction of chondrule structure have shown the heating temperature of the precursor mineral, the number of crystallization and chondrule solidification rate. Precursor minerals in porphyritic chondrules are typically heated below the liquidus temperature of the melt (1,400-1,700 °C), an abundance of seeds is retained and solidification is slow (1-500 °C/h). Barred chondrules are crystallized when heated slightly above the liquidus temperature, when a small number of seeds remain unchanged and when cooling is rapid (500-3,000 °C/h). The chondrules of nonporphyritic (radiated and cryptocrystalline) structures require temperatures much higher than the liquidus temperature, the destruction of all seeds and instant cooling (1000-3000 °C/h) [10, 11].

The porphyritic chondrules of unequilibrated ordinary chondrites (UOC) sometimes contain isolated refractory olivine grains that are considerably enriched in MgO and differ in the isotopic composition of oxygen from the olivine of a chondrule [12, 13] and the higher-Mg nuclei of olivine grains overgrown with lower-Mg forsterite rims [14]. The presence of relict olivine grains in porphyritic chondrules suggests that they were formed by the melting of precursor minerals. Refractory inclusions (CAI and AOA) [15], the fine-grained material of chondrite matrix, as well as the chondrules and fragments of chondrules of previous generations, may behave as precursor material. Other examples are fragments of planetesimals [16], $H_2O$ ice [17, 18], "relict" olivine [19] and clusters of dust [20].

Most ordinary chondrites known on earth show traces of thermal metamorphism. As a result, FeO and MgO concentrations in olivine and low-Ca pyroxene were homogenized on parent chondrite bodies, mesostasis was recrystallized into plagioclase and apatite and chromite were formed. Ordinary chondrites seldom display traces of dissolution and high porosity [21], indicating the involvement of solutions upon thermal metamorphism on the parent bodies of chondrites. Ordinary chondrites are divided into petrological types, based on the presence of well-defined traces of thermal metamorphism and FeO and MgO homogenization. Non-equilibrated ordinary chondrites with no traces of metamorphism are understood as type III. Equilibrated ordinary chondrites are assessed as petrological types IV-VI, based on their thermal metamorphic grade. Equilibrated ordinary chondrites are common, but they are poorly understood, because it was believed that traces of chondrule and planet formation were obliterated by thermal metamorphism [22].

Trace and rare-earth elements are widely used for assessment of the geochemical settings and conditions of formation of genetically different minerals, e.g. zircon [23-25], garnet [26, 27], beryl [28, 29], etc. In addition, the migration of trace elements in olivine and low-Ca pyroxene is poorly affected by thermal and/or impact [30] metamorphism on the parent bodies of chondrites [31, 32]. Therefore, they can be used for the study of early stages in the formation of the Solar System [33] and the study of minerals from equilibrated ordinary chondrites (EOC).

Earlier studies showed that trace elements in EOC minerals remain unequilibrated in meteorites of petrological type V and partly type VI [34]. Trace element distribution in chondrule minerals was not found to depend on the chemical group and petrological type of the meteorite [35].

In our study, we assessed the effect of thermal metamorphism on the mobility of trace elements in the silicate minerals of the porphyritic and radiated chondrules of equilibrated ordinary Kunashak chondrite (L6).


*This is an open access article under the CC BY 4.0 license*

**Analytical methods.**

The Kunashak chondrite sample analyzed (L6) was made available by the Mining Museum of Saint Petersburg Mining University.

The major element chemical composition of minerals was determined using the EPMA method at IGGD RAS on a Jeol JXA-8230 microprobe analyzer with five wave spectrometers. The meteorite substance was placed in a standard epoxy resin mould sprayed with carbon after polishing. Point measurements of mineral compositions were carried out at an accelerating voltage of 20 kV and a current of 20 nA for olivine and pyroxene and at 10 nA for mesostasis. The focused beam was 3 μm in diameter. Natural minerals, pure oxides and metals were used as standards. ZAF algorithm was used for correcting the matrix effect. Kα1 lines were measured for all elements.

Trace and rare-earth element (REE) concentrations in minerals were identified using the secondary ion mass spectrometry (SIMS) method on a Cameca IMS-4f ion microprobe at the Valiev IPT, RAS, Yaroslavl Branch using, the technique described in [36, 37]. The preparation was sprayed with gold prior to measurements. Survey on a Cameca IMS-4f ion microprobe was done under the following conditions: a primary ion beam was $16O_2$, beam diameter was ~ 20 μm; ion current was 5-7 nA; and the accele-rating voltage of the primary beam was 15 keV. The measurement error was no more than 10 % for impurities with concentrations over 1 ppm and 20 % for concentrations of less than 1 ppm. The trace element composition of rock-forming minerals was analyzed as close as possible to the analytical points of major elements using the EPMA method. REE distribution spectra in minerals were CI chondrite-normalized [38].

**Results.**

The Kunashak Meteorite sample contains porphyritic-, barred-, radiated- and granular-structured chondrules varying in size from 1 to 0.5 mm. Chondrule-matrix boundaries are always well-defined, and no metallic rims are present. The matrix consists of coarse olivine and low-Ca pyroxene (clinoenstatite) grains. High-Ca pyroxene (augite-diopside), plagioclase of oligoclase composition, apatite, chromite, kamacite-taenite and troilite. The matrix has melting pockets and fractures filled with ore minerals. The matrix and chondrules of the meteorite are highly porous. No minerals produced by earth weathering have been found.

When studying the trace element composition of chondrule minerals, we analyzed porphyritic olivine 8PO-1 and olivine-pyroxenitic 8POP-3 chondrules, as well as radiated olivine-pyroxenitic chondrule 8ROP-2 (Fig.1). Chondrules 8PO-1 and

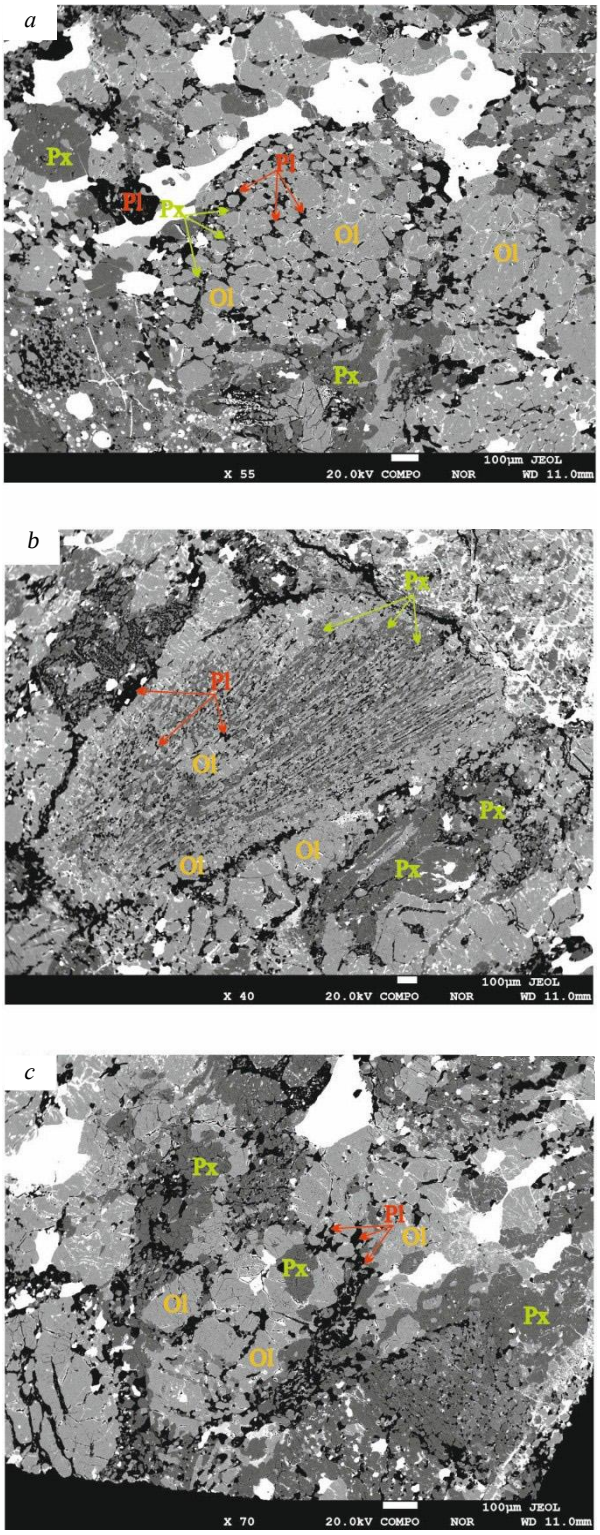



Fig.1. BSE images of chondrules of the Kunashak Meteorite:
*a* – 8PO-1; *b* – 8ROP-2; *c* – 8POP-3;
Ol – olivine, Px – low-Ca pyroxene, Pl – plagioclase



*This is an open access article under the CC BY 4.0 license*

8ROP-2 are about 1 mm in size and show well-defined chondrule-matrix boundaries. Chondrule 8POP-3 is smaller (0.5 mm) and shows indistinct boundaries. The chondrules have no metallic rims, but 8ROP-2 has an olivine rim along the perimeter.

Chondrule 8PO-1 consists of small (100 μm on the average) isometric olivine grains, scarce small (less than 50 μm) xenomorphic low-Ca pyroxene and plagioclase grains (Fig.1, *a*). Coarse (300-500 μm) olivine, pyroxene and plagioclase grains are present in the matrix, near the chondrule. Ore mineral streaks are scarce.

Olivine in porphyritic chondrule 8PO-1 was recognized as forsterite (Fo 75). It is present as a coarse grain in the centre of the chondrule and small grains throughout the chondrule. Idiomorphic olivine grains do not contact each other within the chondrule. No well-defined fractures and pores in the grains were found. The composition of major elements in olivine is homogeneous. There are no differences between olivine in the centre and olivine on the margin of the chondrule, as well as olivine in the meteorite matrix, near the chondrule (Table 1).

*Table 1*

**Major (wt.%) and trace (ppm) element composition of silicate minerals from 8PO-1 chondrule of the Kunashak Meteorite**

| Element | Olivine | | | Pyroxene | | | Plagioclase | | |
|---|---|---|---|---|---|---|---|---|---|
| | Centre | Rim | Matrix | Centre | Rim | Matrix | Centre | Rim | Matrix |
| $SiO_2$ | 38.73 | 38.63 | 38.89 | 55.39 | 55.91 | 55.07 | 65.53 | 65.21 | 65.61 |
| $Al_2O_3$ | 0.01 | 0.01 | b.d.l. | 0.29 | 0.15 | 0.31 | 21.07 | 21.20 | 21.19 |
| MgO | 38.74 | 38.70 | 39.31 | 28.12 | 28.22 | 28.04 | 0.06 | 0.17 | 0.04 |
| $TiO_2$ | 0.04 | 0.01 | 0.03 | 0.33 | 0.21 | 0.41 | 0.01 | 0.02 | 0.02 |
| CaO | 0.02 | 0.03 | 0.02 | 0.82 | 0.76 | 1.04 | 2.19 | 2.40 | 2.24 |
| FeO | 22.72 | 22.89 | 22.37 | 14.08 | 13.90 | 13.77 | 0.66 | 0.64 | 0.32 |
| MnO | 0.44 | 0.43 | 0.42 | 0.48 | 0.46 | 0.45 | – | – | – |
| $Cr_2O_3$ | b.d.l. | 0.08 | 0.01 | 0.16 | 0.09 | 0.26 | – | – | – |
| NiO | b.d.l. | 0.03 | 0.02 | 0.01 | b.d.l. | b.d.l. | – | – | – |
| $Na_2O$ | – | – | – | 0.04 | b.d.l. | b.d.l. | 10.36 | 9.95 | 10.02 |
| $K_2O$ | – | – | – | b.d.l. | b.d.l. | b.d.l. | 0.75 | 0.99 | 0.93 |
| Total | 100.69 | 100.80 | 101.07 | 99.72 | 99.71 | 99.34 | 100.63 | 100.59 | 100.35 |
| Zr | 1.29 | 2.39 | 0.75 | 61.2 | 4.29 | 1.91 | 2.32 | 1.15 | 7.00 |
| Hf | 0.05 | 0.05 | 0.06 | 1.61 | 0.12 | 0.08 | 0.13 | 0.04 | 0.16 |
| Ca | 4,531 | 4,665 | 4,715 | 7,266 | 6,018 | 6,373 | – | – | – |
| Y | 0.06 | 0.12 | 0.07 | 0.48 | 0.41 | 0.32 | 0.11 | 0.15 | 1.11 |
| Al | 39.5 | 172 | 61.6 | 283 | 536 | 585 | – | – | – |
| Ti | 241 | 136 | 99.2 | 186 | 986 | 1,306 | 226 | 250 | 1,101 |
| Nb | 2.27 | 0.46 | 0.17 | 0.69 | 0.45 | 0.11 | 0.42 | 0.17 | 0.68 |
| La | 0.05 | 0.14 | 0.08 | 1.93 | 0.12 | 0.04 | 0.09 | 0.08 | 0.77 |
| Ce | 0.11 | 0.12 | 0.09 | 8.00 | 0.25 | 0.19 | 0.12 | 0.14 | 1.16 |
| Pr | 0.01 | 0.04 | 0.02 | 0.40 | 0.02 | 0.02 | 0.02 | 0.02 | 0.23 |
| Nd | 0.07 | 0.11 | 0.06 | 2.16 | 0.05 | 0.08 | 0.13 | 0.04 | 0.64 |
| Sm | 0.02 | 0.02 | b.d.l. | 0.31 | 0.12 | b.d.l. | b.d.l. | b.d.l. | 0.12 |
| Eu | 0.01 | b.d.l. | 0.01 | 0.06 | 0.03 | 0.01 | 0.27 | 0.38 | 0.23 |
| Gd | 0.02 | 0.05 | 0.03 | 1.31 | 0.10 | b.d.l. | 0.01 | 0.02 | 0.26 |
| Dy | b.d.l. | 0.03 | 0.02 | 0.05 | 0.05 | 0.05 | b.d.l. | 0.02 | 0.19 |
| Er | 0.02 | 0.03 | b.d.l. | 0.06 | 0.07 | 0.07 | b.d.l. | 0.14 | 0.14 |
| Yb | 0.03 | 0.02 | 0.03 | 0.08 | 0.10 | 0.11 | 0.04 | 0.04 | 0.16 |
| Lu | b.d.l. | 0.01 | 0.01 | 0.03 | 0.01 | 0.02 | 0.01 | 0.01 | 0.03 |
| Sr | 0.18 | 0.40 | 0.16 | 1.06 | 0.55 | 0.25 | 51.2 | 71.7 | 35.5 |
| Ba | 0.18 | 0.51 | 0.23 | 5.09 | 0.51 | 0.38 | 26.5 | 36.9 | 7.05 |



*This is an open access article under the CC BY 4.0 license*

End of Table 1

| Element | Olivine | | | Pyroxene | | | Plagioclase | | |
|---|---|---|---|---|---|---|---|---|---|
| | Centre | Rim | Matrix | | Centre | Rim | Matrix | | Centre |
| V | 18.2 | 18.5 | 18.8 | 33.7 | 41.0 | 50.4 | 28.4 | 13.5 | 53.7 |
| Ni | 40.0 | 94.6 | 35.0 | 193 | 298 | 104 | – | – | – |
| Cr | 520 | 503 | 436 | 1,180 | 809 | 991 | 792 | 35.2 | 1,176 |
| Rb | 1.39 | 1.59 | 1.76 | 2.46 | 1.44 | 0.84 | 7.21 | 9.22 | 2.91 |
| REE | 0.36 | 0.57 | 0.35 | 14.4 | 0.93 | 0.60 | 0.69 | 0.88 | 3.92 |
| LREE | 0.29 | 0.44 | 0.26 | 12.9 | 0.60 | 0.35 | 0.63 | 0.65 | 3.15 |
| HREE | 0.07 | 0.13 | 0.09 | 1.53 | 0.33 | 0.26 | 0.06 | 0.22 | 0.77 |

*Note.* Empty cell – no element detected; b.d.l. – element content is below the detection limit.

The composition of trace elements in the olivine of chondrule 8PO-1 is also homogeneous. Nb concentration decreases from the centre of the chondrule (2.26 ppm) to the margin (0.46 ppm) and matrix (0.17 ppm) of the meteorite. Trace element concentrations are below chondrite values. The trace element distribution spectrum is subhorizontal (Fig.2, *a*).

Refractory trace element concentrations in the olivine of chondrule 8 PO-1 exceeds unequilibrated chondrite concentrations in olivine [39], except for Al, and fully coincides with respect to volatile elements (Sr, Ba and Ni).

The low-Ca pyroxene of chondrule 8PO-1 seldom occurs in the chondrule. It does not form its own grains and usually grows on olivine grains. Pyroxene is present as small (50 μm) xenomorphic aggregates and has much in common with plagioclase. Low-Ca pyroxene is present as clinoenstatite (En 76, Wo 1-2). It shows no significant variations in major element composition. However, low-Ca pyroxene in the matrix contains more $TiO_2$, CaO and $Cr_2O_3$ than pyroxene in the centre and on the margin of the chondrule (Table 1).

Trace element concentrations in low-Ca pyroxene from chondrule 8PO-1 decreases from the centre to the margin of the chondrule and the matrix of the meteorite. Pyroxene in the centre of the chondrule is richer in all refractory elements (Zr, Hf, Nb, LREE), as well as in Sr and Ba, than pyroxene on the margin and in the matrix of the meteorite. Pyroxene on the chondrule margin shows intermediate concentrations of the above elements in comparison with the centre of the chondrule centre and the matrix of the meteorite, while pyroxene in the matrix is impoverished in them.

The trace element composition of low-Ca pyroxene is consistent with chondrite values, so that trace element composition in unequilibrated ordinary chondrites is exceeded. The rare earth element distribution spectrum is poorly differentiated, but it shows the prevalence of LREE over HREE, especially in pyroxene from the centre of the chondrule (Fig.2, *b*).

Plagioclase in chondrule 8PO-1 is scarce. It commonly occurs as small xenomorphic aggregates filling interstices between olivine and pyroxene. Plagioclase in the chondrule is present as oligoclase (An 10-11, Or 5-4). Major element composition remains unchanged (Table 1).

Trace element concentrations in plagioclase are highly heterogeneous. Plagioclase in the matrix is richer in trace elements and REE than plagioclase in the chondrule. Plagioclase on the chondrule margin is poor in Zr, Hf and Nb. Plagioclase in the centre of the chondrule occupies an intermediate position.

The trace element distribution spectrum shows trace element concentrations consistent with chondrite values (Fig.2, *c*). Plagioclase in the matrix mainly coincides with the spectrum of plagioclase for Vigarano Meteorite, although it is slightly impoverished in HREE. The spidergram for plagioclase in the chondrule is similar to the diagram of plagioclase for Renazzo Meteorite.

Radiated chondrule 8ROP-2 consists of fine elongated skeletal olivine and low-Ca pyroxene crystals extending from a common centre. The ~1 mm chondrule is oval in shape and has a



*This is an open access article under the CC BY 4.0 license*

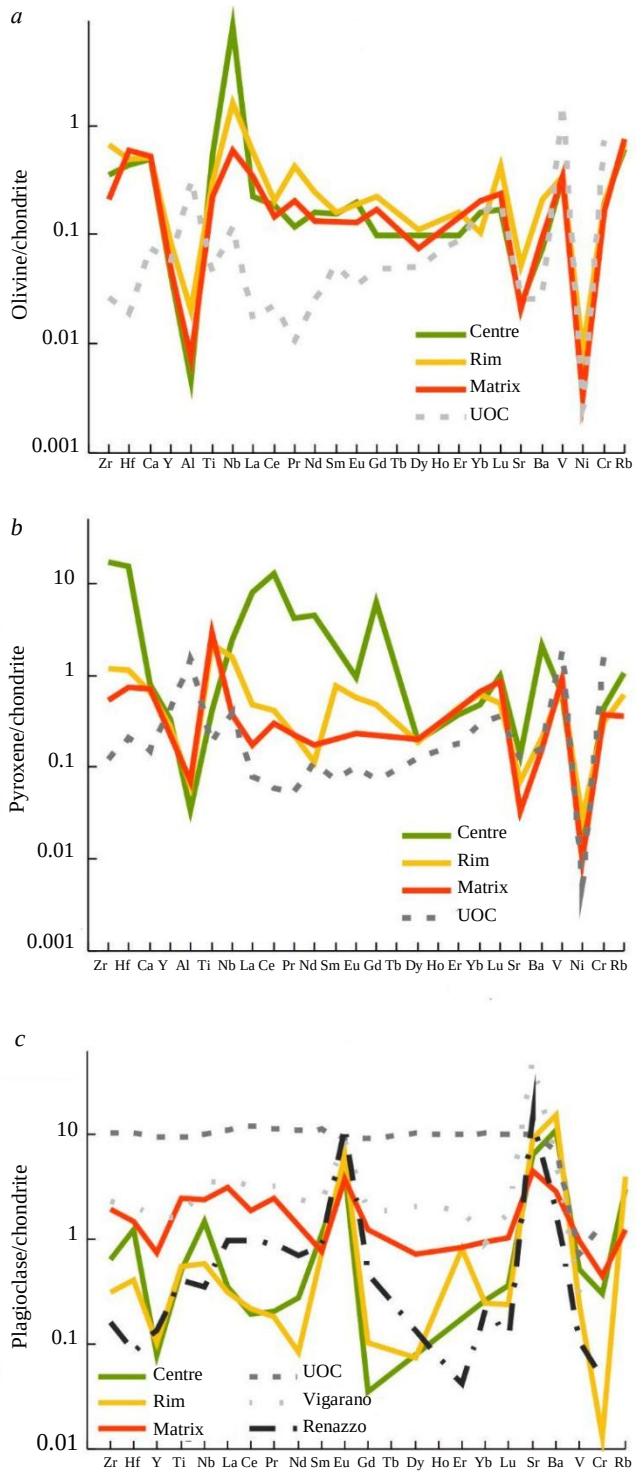



Fig.2. Spider diagrams for trace elements normalized to CI chondrite. Chondrule 8PO-1: olivine (*a*); low-Ca pyroxene (*b*) and mesostasis (*c*). Data on the composition of UOC, Vigarano and Renazzo minerals are given according [38, 40]

well-defined boundary with matrix and an olivine along the perimeter. On the wide side, it is bounded by a fracture and a melting pocket with abundant ore streaks (see Fig.1, *b*).

Olivine in chondrule 8ROP-2 forms thin (up to 100 μm in width) elongated beams extending from one chondrule margin to the other from a common centre. The olivine grains are homogeneous, have no fractures and are often overgrown with ore minerals. Olivine in the chondrule is present as forsterite (Fo 75). The major element composition is homogeneous (Table 2).

The trace element composition of olivine in chondrule 8ROP-2 varies with the position of the analytical point. Olivine in the centre of the chondrule is poorer in HREE than olivine on the chondrule margin and in the meteorite matrix. Olivine in the meteorite matrix has minimum Al concentration (54.5 ppm).

The trace element distribution spectrum for olivine in chondrule 8ROP-2 is poorly differentiated. HREE does not prevail over LREE (Fig.3, *a*). Trace element concentrations in the olivine of the chondrule are below chondrite values, but exceed refractory element concentrations in the porphyritic chondrules of unequilibrated ordinary chondrites.

Low-Ca pyroxene in chondrule 8ROP-2 is present as clinoenstatite (En 76, Wo 1). Its major element concentrations are constant, although pyroxene in the matrix is poor in impurity elements ($Al_2O_3$, $TiO_2$, CaO, $Cr_2O_3$) (Table 2). Low-Ca pyroxene seldom occurs in chondrules. It commonly overgrows skeletal olivine crystals. It often occurs as fine (up to 50 μm) xenomorphic aggregates.

Low-Ca pyroxene in the centre of chondrule 8ROP-2 contains higher trace element concentrations than pyroxene on the chondrule margin and in the matrix of the meteorite. Pyroxene on the chondrule margin and in the matrix of the meteorite has similar trace element concentrations, but pyroxene on the chondrule margin has minimum moderately volatile Sr and Ba concentrations.

The trace element distribution spectrum for low-Ca pyroxene in chondrule 8ROP-2 displays chondrite values, slightly exceeding trace element concentrations in pyroxene from the chondrules of unequilibrated ordinary chondrites (Fig.3, *c*). Low-Ca pyroxene in chondrule 8ROP-2 contains more Ti than UOC. The rare-earth distribution spectrum shows that HREE clearly dominates over LREE in the low-Ca pyroxene of chondrule ROP-2.

Plagioclase in chondrule 8ROP-2 is present as oligoclase (An 10-12, Or 4). Albite grains (An 9, Or 5) occur in the matrix (Table 2). In the chondrule, plagioclase fills small (~10 μm)



This is an open access article under the CC BY 4.0 license

interstices between olivine and pyroxene and, therefore, cannot be studied. Major element composition in plagioclase is permanent, although minor variations in impurity element (Mg, Fe) concentrations take place.

*Table 2*

**Major (wt.%) and trace (ppm) element composition of silicate minerals from 8ROP-2 chondrule of the Kunashak Meteorite**

| Element | Olivine | | | Pyroxene | | | Plagioclase | | |
|---|---|---|---|---|---|---|---|---|---|
| | Centre | Rim | Matrix | Centre | Rim | Matrix | Centre | Matrix | Matrix |
| $SiO_2$ | 38.75 | 38.30 | 38.22 | 55.22 | 55.07 | 55.91 | 65.63 | 65.70 | 65.18 |
| $Al_2O_3$ | 0.01 | 0.02 | b.d.l. | 0.40 | 0.37 | 0.15 | 21.13 | 21.21 | 21.01 |
| MgO | 38.81 | 39.27 | 39.21 | 28.28 | 28.07 | 28.53 | 0.13 | 0.09 | 0.10 |
| $TiO_2$ | 0.02 | 0.01 | 0.00 | 0.46 | 0.39 | 0.20 | 0.03 | 0.02 | 0.03 |
| CaO | 0.02 | 0.02 | 0.02 | 0.84 | 0.87 | 0.63 | 2.66 | 2.32 | 2.07 |
| FeO | 22.85 | 22.22 | 22.77 | 13.70 | 14.65 | 14.05 | 0.72 | 0.40 | 0.52 |
| MnO | 0.48 | 0.50 | 0.46 | 0.45 | 0.48 | 0.48 | – | – | – |
| $Cr_2O_3$ | 0.02 | 0.02 | 0.01 | 0.22 | 0.24 | 0.09 | – | – | – |
| NiO | b.d.l. | 0.01 | b.d.l. | 0.02 | 0.09 | 0.02 | – | – | – |
| $Na_2O$ | – | – | – | 0.02 | b.d.l. | 0.01 | 9.47 | 10.28 | 10.20 |
| $K_2O$ | – | – | – | b.d.l. | 0.02 | b.d.l. | 0.71 | 0.88 | 0.99 |
| Total | 100.96 | 100.37 | 100.68 | 99.61 | 100.23 | 100.07 | 100.49 | 100.89 | 100.09 |
| Zr | 0.67 | 0.81 | 0.57 | 19.6 | 3.13 | 1.16 | 44.1 | 4.43 | 6.96 |
| Hf | b.d.l. | 0.06 | b.d.l. | 0.49 | 0.10 | 0.04 | 0.95 | 0.24 | 0.16 |
| Ca | 5,658 | 5,122 | 5,208 | 27,607 | 6,545 | 6,374 | – | – | – |
| Y | 0.03 | 0.09 | 0.08 | 2.21 | 0.50 | 0.29 | 0.30 | 0.34 | 1.10 |
| Al | 236 | 1,055 | 54.6 | 8,825 | 1,395 | 613 | – | – | – |
| Ti | 88.6 | 113 | 55.1 | 1,240 | 2,555 | 1,245 | 422 | 624 | 1,094 |
| Nb | 0.37 | 0.36 | 0.06 | 1.47 | 0.32 | 0.13 | 0.59 | 0.77 | 0.68 |
| La | 0.03 | 0.02 | 0.05 | 0.14 | 0.06 | 0.02 | 1.63 | 0.13 | 0.77 |
| Ce | 0.07 | 0.09 | 0.08 | 0.44 | 0.10 | 0.20 | 1.60 | 0.25 | 1.15 |
| Pr | 0.01 | 0,01 | 0.02 | 0.05 | 0.01 | 0.01 | 0.38 | 0.04 | 0.23 |
| Nd | 0.06 | 0.05 | 0.06 | 0.32 | 0.05 | 0.05 | 1.23 | 0.11 | 0.64 |
| Sm | b.d.l. | 0.05 | b.d.l. | 0.10 | 0.03 | 0.03 | 0.13 | b.d.l. | 0.12 |
| Eu | 0.00 | 0.01 | 0.01 | 0.04 | 0.02 | 0.01 | 0.63 | 0.05 | 0.22 |
| Gd | 0.03 | 0.09 | 0.06 | 0.15 | 0.06 | 0.05 | 0.19 | 0.05 | 0.26 |
| Dy | 0.01 | 0.04 | 0.04 | 0.32 | 0.05 | 0.04 | 0.03 | 0.05 | 0.19 |
| Er | b.d.l. | 0.03 | 0.04 | 0.33 | 0.03 | 0.04 | 0.06 | 0.09 | 0.14 |
| Yb | 0.01 | 0.04 | 0.09 | 0.34 | 0.22 | 0.13 | 0.07 | 0.07 | 0.16 |
| Lu | 0.01 | 0.01 | 0.01 | 0.04 | 0.02 | 0.01 | 0.02 | 0.04 | 0.03 |
| Sr | 0.44 | 1.14 | 0.19 | 10.8 | 0.17 | 1.32 | 109 | 6.76 | 35.3 |
| Ba | 0.42 | 0.66 | 0.29 | 4.11 | 0.13 | 0.22 | 27.3 | 2.47 | 7.00 |
| V | 23.2 | 20.5 | 18.2 | 117 | 82.9 | 49.7 | 18.5 | 38.5 | 53.3 |
| Ni | 45.3 | 49.9 | 44.0 | 110 | 370 | 286 | – | – | – |
| Cr | 889 | 520 | 472 | 1,672 | 1,582 | 884 | 168 | 587 | 1,168 |
| Rb | 2.06 | 2.58 | 1.46 | 3.18 | 1.01 | 0.59 | 13.1 | 8.81 | 2.89 |
| REE | 0.24 | 0.45 | 0.45 | 2.27 | 0.65 | 0.60 | 5.98 | 0.88 | 3.90 |
| LREE | 0.17 | 0.24 | 0.22 | 1.09 | 0.27 | 0.33 | 5.61 | 0.58 | 3.13 |
| HREE | 0.07 | 0.21 | 0.24 | 1.19 | 0.39 | 0.27 | 0.37 | 0.30 | 0.77 |



*This is an open access article under the CC BY 4.0 license*

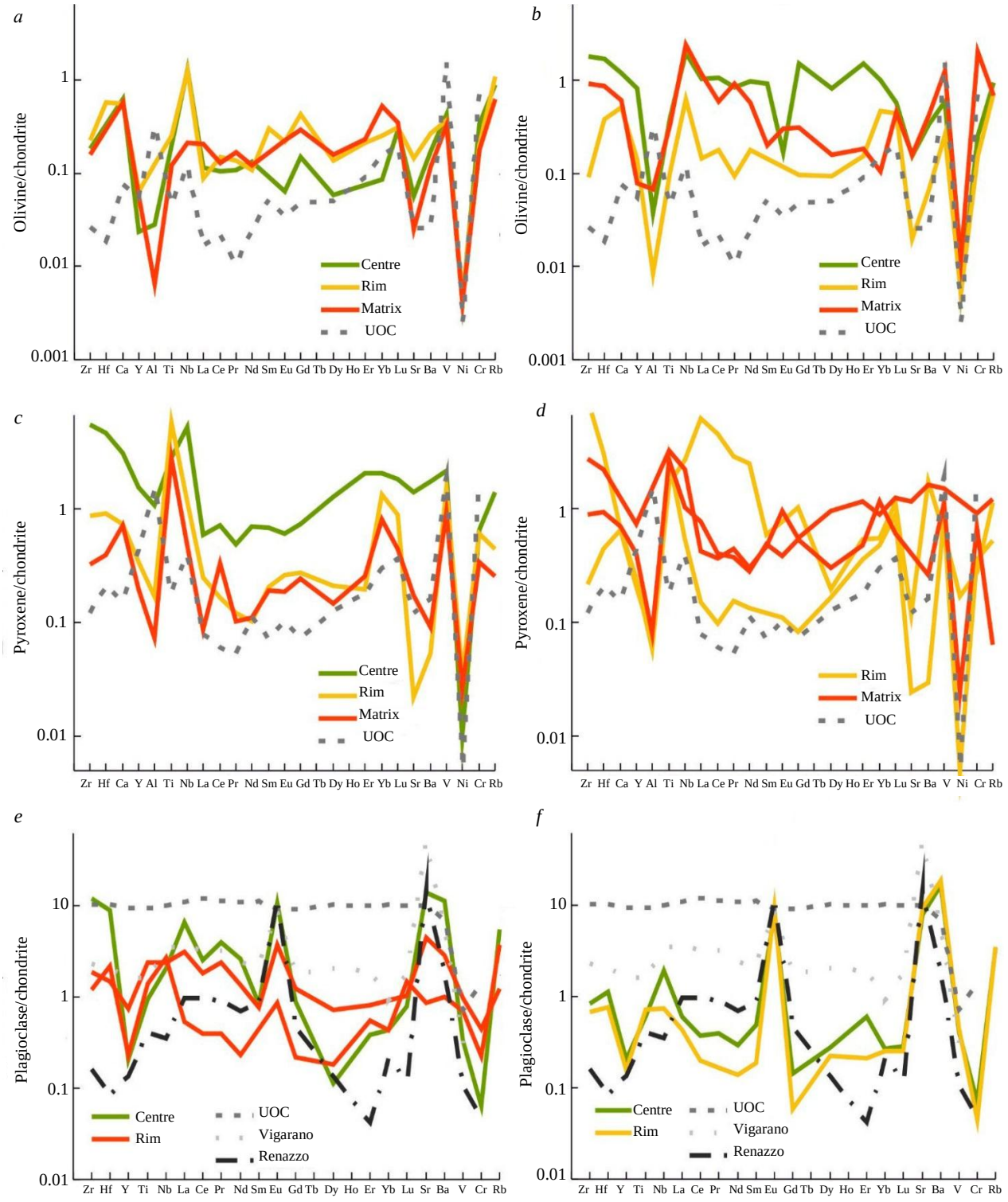



Fig.3. Spider diagrams for trace elements normalized to CI chondrite.
Chondrule 8ROP-2: olivine (*a*); low-Ca pyroxene (*c*) and mesostasis (*e*);
chondrule 8POP-3: olivine (*b*); low-Ca pyroxene (*d*) and mesostasis (*f*).
Data on the composition of UOC, Vigarano and Renazzo minerals are given according [38, 40]

Trace element concentrations in plagioclase from chondrule 8ROP-2 are heterogeneous. In the centre of the chondrule, plagioclase is richer in trace elements than plagioclase in the matrix, except for HREE. In the matrix, plagioclase grains contain various trace element concentrations, although the trace element distribution spectra resemble each other (Fig.3, *e*). Trace element concentrations in the plagioclase of chondrule 8ROP-2 and in the matrix are above chondrite values.



*This is an open access article under the CC BY 4.0 license*

The trace element distribution spectra in chondrule 8ROP-2 are more similar to plagioclase in Renazzo coaly chondrite [38, 40], but refractory and rare-earth element concentrations are higher. The distribution spectra are poorly differentiated, a well-defined europium anomaly is present and LREE prevails over HREE in plagioclase from the centre of the chondrule.

Porphyritic olivine-pyroxene chondrule 8POP-3 (see Fig.1, *c*), 0.5 mm in size, contains coarse olivine and plagioclase grains and has an obliterated boundary with the matrix. Occurring near the chondrule is a plagioclase-olivine aggregate showing the integrated xenomorphic manifestation of plagioclase, which contains fine (up to 50 μm by elongation) elongated olivine grains.

In chondrule 8POP-3, olivine is present as forsterite (Fo 75). Its major element composition is stable (Table 3). Olivine makes up the bulk of chondrule POP-3, occurring as coarse (200-300 μm) idiomorphic grains. It looks homogeneous and slightly fractured on BSE-images.

The trace element composition of olivine is heterogeneous. In the centre of the chondrule, olivine is richer in refractory elements than olivine on the margin and in the matrix of the meteorite. Olivine on the chondrule margin contains the lowest trace element concentrations. Olivine in the matrix occupies an intermediate position.

Trace element concentrations are consistent with chondrite values. They exceed refractory and rare-earth element concentrations in porphyritic chondrule olivine from unequilibrated ordinary chondrite (Fig.3, *b*). The trace element distribution in the olivine of chondrule 8POP-3 is poorly differentiated. LREE prevails over HREE in olivine from the matrix.

Low-Ca pyroxene in chondrule 8POP-3 is less common than olivine, making up no more than 10 % of the chondrule. Pyroxene is present as fine (up to 200 μm) xenomorphic grains occasionally growing on fine olivine grains. In back-scattered electrons, it looks homogeneous and has no fractures. Low-Ca pyroxene is present as clinoenstatite (En 76-77, Wo 1-2). Its major element composition is homogeneous, but impurity element (Ti, Cr) concentrations vary slightly (Table 3).

*Table 3*

**Major (wt.%) and trace (ppm) element composition of silicate minerals from 8POP-3 chondrule of the Kunashak Meteorite**

| Element | Olivine | | | Pyroxene | | | | Plagioclase | |
|---|---|---|---|---|---|---|---|---|---|
| | Centre | Rim | Matrix | Rim | Rim | Matrix | Matrix | Centre | Rim |
| $SiO_2$ | 38.32 | 38.05 | 38.73 | 56.38 | 56.32 | 56.17 | 55.49 | 63.63 | 65.44 |
| $Al_2O_3$ | b.d.l. | 0.02 | b.d.l. | 0.16 | 0.12 | 0.16 | 0.17 | 20.25 | 20.96 |
| MgO | 38.75 | 38.60 | 38.64 | 28.56 | 28.68 | 28.44 | 28.27 | 0.99 | 0.18 |
| $TiO_2$ | b.d.l. | b.d.l. | 0.04 | 0.20 | 0.13 | 0.19 | 0.20 | b.d.l. | 0.04 |
| CaO | 0.05 | 0.05 | 0.05 | 0.86 | 0.86 | 0.75 | 1.05 | 3.66 | 2.43 |
| FeO | 22.87 | 22.37 | 22.44 | 13.83 | 13.52 | 13.97 | 13.87 | 1.57 | 0.43 |
| MnO | 0.49 | 0.50 | 0.42 | 0.46 | 0.48 | 0.49 | 0.42 | – | – |
| $Cr_2O_3$ | b.d.l. | 0.02 | 0.03 | 0.12 | 0.11 | 0.14 | 0.15 | – | – |
| NiO | 0.01 | b.d.l. | b.d.l. | b.d.l. | b.d.l. | 0.01 | b.d.l. | – | – |
| $Na_2O$ | – | – | – | 0.03 | b.d.l. | 0.04 | 0.02 | 9.60 | 10.10 |
| $K_2O$ | – | – | – | 0.00 | 0.01 | 0.01 | 0.01 | 0.87 | 0.78 |
| Total | 100.49 | 99.60 | 100.35 | 100.58 | 100.23 | 100.35 | 99.65 | 100.57 | 100.36 |
| Zr | 6.55 | 0.32 | 3.35 | 0.78 | 32.7 | 9.89 | 3.22 | 3.06 | 2.48 |
| Hf | 0.18 | 0.04 | 0.09 | 0.05 | 0.32 | 0.23 | 0.10 | 0.12 | 0.08 |
| Ca | 11,012 | 4,690 | 5,527 | 5,877 | 6,012 | – | 6,332 | – | – |
| Y | 1.20 | 0.21 | 0.12 | 0.30 | 0.35 | 1.06 | 0.57 | 0.31 | 0.23 |
| Al | 314 | 71.4 | 565 | 591 | 489 | – | 670 | – | – |
| Ti | 175 | 46.2 | 147 | 1,214 | 730 | 1,426 | 1,177 | 276 | 327 |



*This is an open access article under the CC BY 4.0 license*

End of Table 3

| Element | Olivine | | | Pyroxene | | | | Plagioclase | |
|---|---|---|---|---|---|---|---|---|---|
| | Centre | Rim | Matrix | Rim | Rim | Matrix | Matrix | Centre | Rim |
| Nb | 0.56 | 0.18 | 0.68 | 0.15 | 0.76 | 0.61 | 0.29 | 0.56 | 0.21 |
| La | 0.25 | 0.04 | 0.28 | 0.04 | 1.46 | 0.10 | 0.18 | 0.15 | 0.11 |
| Ce | 0.66 | 0.11 | 0.36 | 0.06 | 2.79 | 0.23 | 0.25 | 0.23 | 0.12 |
| Pr | 0.08 | 0.01 | 0.09 | 0.01 | 0.26 | 0.04 | 0.03 | 0.04 | 0.02 |
| Nd | 0.46 | 0.08 | 0.27 | 0.06 | 1.18 | 0.14 | 0.13 | 0.14 | 0.07 |
| Sm | 0.14 | b.d.l. | 0.03 | b.d.l. | 0.09 | 0.07 | 0.07 | 0.08 | 0.03 |
| Eu | 0.01 | b.d.l. | 0.02 | 0.01 | 0.04 | 0.06 | 0.02 | 0.47 | 0.56 |
| Gd | 0.31 | 0.02 | 0.06 | 0.02 | 0.21 | 0.11 | 0.11 | 0.03 | 0.01 |
| Dy | 0.21 | 0.02 | 0.04 | 0.04 | 0.05 | 0.24 | 0.08 | 0.07 | 0.06 |
| Er | 0.25 | 0.03 | 0.03 | 0.06 | 0.09 | 0.19 | 0.08 | 0.10 | 0.04 |
| Yb | 0.17 | 0.08 | 0.02 | 0.08 | 0.09 | 0.15 | 0.19 | 0.05 | 0.04 |
| Lu | 0.01 | 0.01 | 0.01 | 0.02 | 0.03 | 0.03 | 0.01 | 0.01 | 0.01 |
| Sr | 1.20 | 0.15 | 1.23 | 0.19 | 0.92 | 8.84 | 3.13 | 63.0 | 73.7 |
| Ba | 0.82 | 0.16 | 1.05 | 0.07 | 4.17 | 3.87 | 0.62 | 40.7 | 46.6 |
| V | 32.4 | 14.2 | 68.8 | 45.8 | 33.0 | 81.0 | 60.4 | 22.6 | 24.6 |
| Ni | 56.1 | 55.7 | 127 | 53.6 | 1,813 | – | 260 | – | – |
| Cr | 665 | 407 | 5,290 | 922 | 717 | 2,328 | 1,786 | 185 | 117 |
| Rb | 2.21 | 1.67 | 1.59 | 1.20 | 2.59 | 2.79 | 0.15 | 7.92 | 8.21 |
| REE | 2.56 | 0.40 | 1.22 | 0.40 | 6.30 | 1.35 | 1.17 | 1.36 | 1.06 |
| LREE | 1.60 | 0.24 | 1.05 | 0.18 | 5.83 | 0.64 | 0.69 | 1.11 | 0.90 |
| HREE | 0.96 | 0.16 | 0.16 | 0.22 | 0.47 | 0.72 | 0.47 | 0.25 | 0.16 |

Trace element concentrations are fairly heterogeneous in low-Ca pyroxene from chondrule 8POP-3. Grains with very high and very low LREE concentrations, relative to those in the pyroxene of the matrix, occur in the pyroxene of the chondrule margin. Pyroxene in the matrix is richer in Y, Sr and Ba than pyroxene in the chondrule. It occupies an intermediate position with respect to REE concentration.

The trace element distribution spectrum in low-Ca pyroxene from chondrule 8POP-3 is highly differentiated and is consistent with chondrite values (Fig.3, *d*). Trace element concentrations in low-Ca pyroxene from chondrule 8POP-3 are higher than those in the pyroxene of porphyritic chondrules in unequilibrated ordinary chondrites.

Plagioclase in chondrule 8POP-3 is present as oligoclase (An 10-16, Or 4) with high variable impurity element (CaO, MgO, FeO) composition (Table 3). Plagioclase in chondrule 8POP-3 occurs in interstices between olivine and pyroxene. It is not abundant in the chondrule, forming aggregates no more than 50 μm in size.

Trace element concentrations in the plagioclase of chondrule 8POP-3 are homogeneous. Trace element concentrations in plagioclase are consistent with chondrite values, coinciding with plagioclase in Renazzo coaly chondrite (Fig.3, *f*). The distribution spectra are poorly differentiated. They display a well-defined europium anomaly and show no prevalence of LREE over HREE.

**Discussion.**

The silicate minerals of porphyritic (8PO-1, 8POP-3) and radiated (8ROP-2) chondrules do not differ in major element concentrations but differ in the trace element composition of these minerals.

The trace element distribution spectrum for olvine in chondrules is poorly differentiated, but some grains of porphyritic chondrule 8POP-3 are enriched in incompatible LREE, Sr and Ba (Fig.4, *a*). Olivine in this chondrule is more abundant than olivine in other chondrules, presumably indicating a relationship between grain size and trace element concentration. No considerable differences in the trace element composition of mineral grains occurring inside the chondrule or in the meteorite matrix were found (Fig.4, *b*).



*This is an open access article under the CC BY 4.0 license*

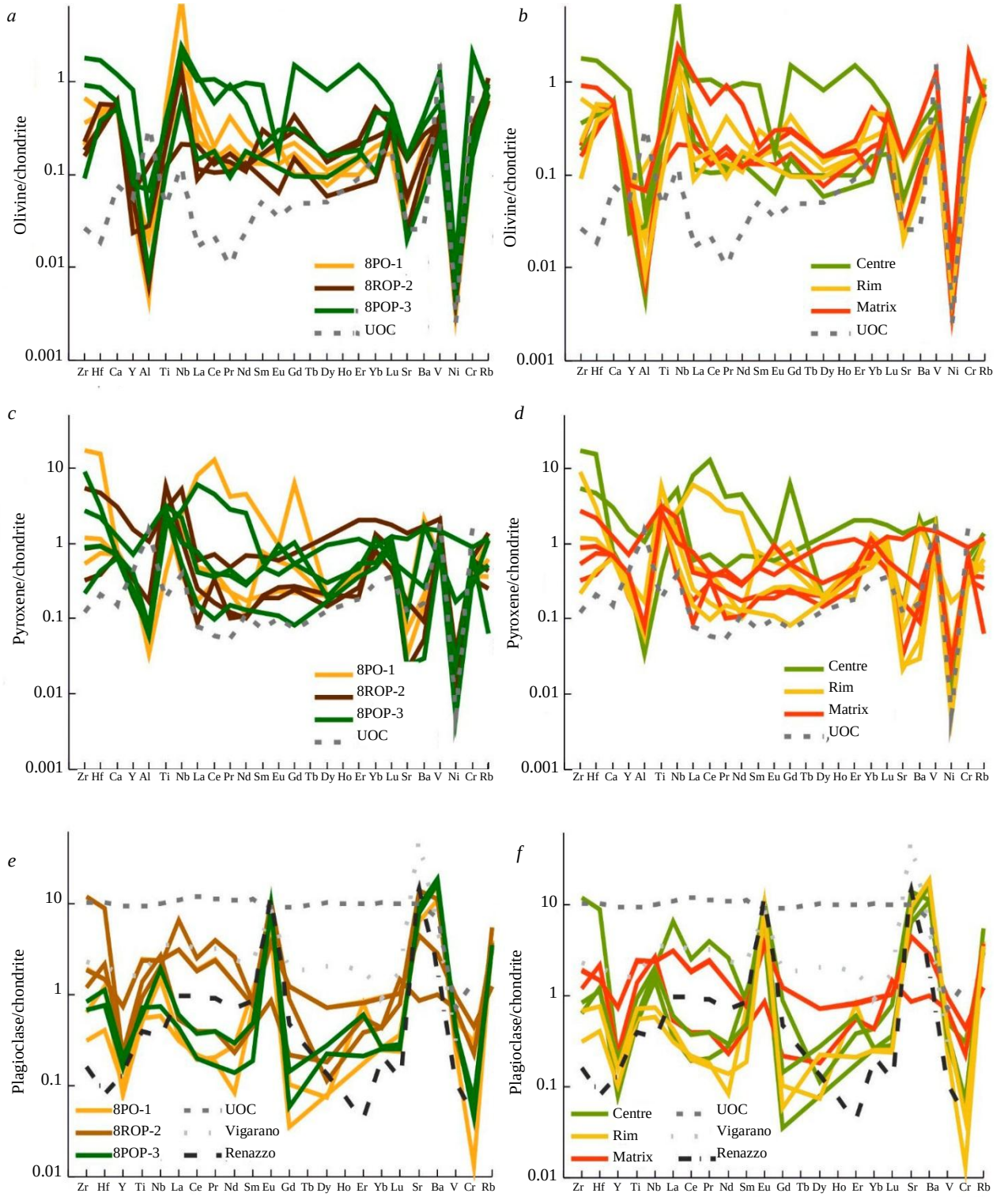



Fig.4. Spider diagrams for trace elements normalized to CI chondrite in olivine, low-Ca pyroxene and plagioclase from the Kunashak Meteorite: relative to different chondrules (*a*, *c*, *e*) and the location of grains inside/outside the chondrule (*b*, *d*, *f*). Data on the composition of UOC, Vigarano and Renazzo minerals are given according to [38, 40]

Differences between olivine in the chondrules in diagrams showing Rb-Yb (Fig.5, *a*) and Zr-Ti relationships (Fig.5, *b*) are better defined than those in trace element distribution spectra. For instance, Rb-Yb relationship shows that olivine in chondrule 8ROP-2 is enriched in moderately volatile and incompatible Rb, while olivine in porphyritic olivine-pyroxene chondrule 8POP-3 is enriched in refractory Yb. Olivine in chondrule 8PO-1 is poor in these elements.



*This is an open access article under the CC BY 4.0 license*

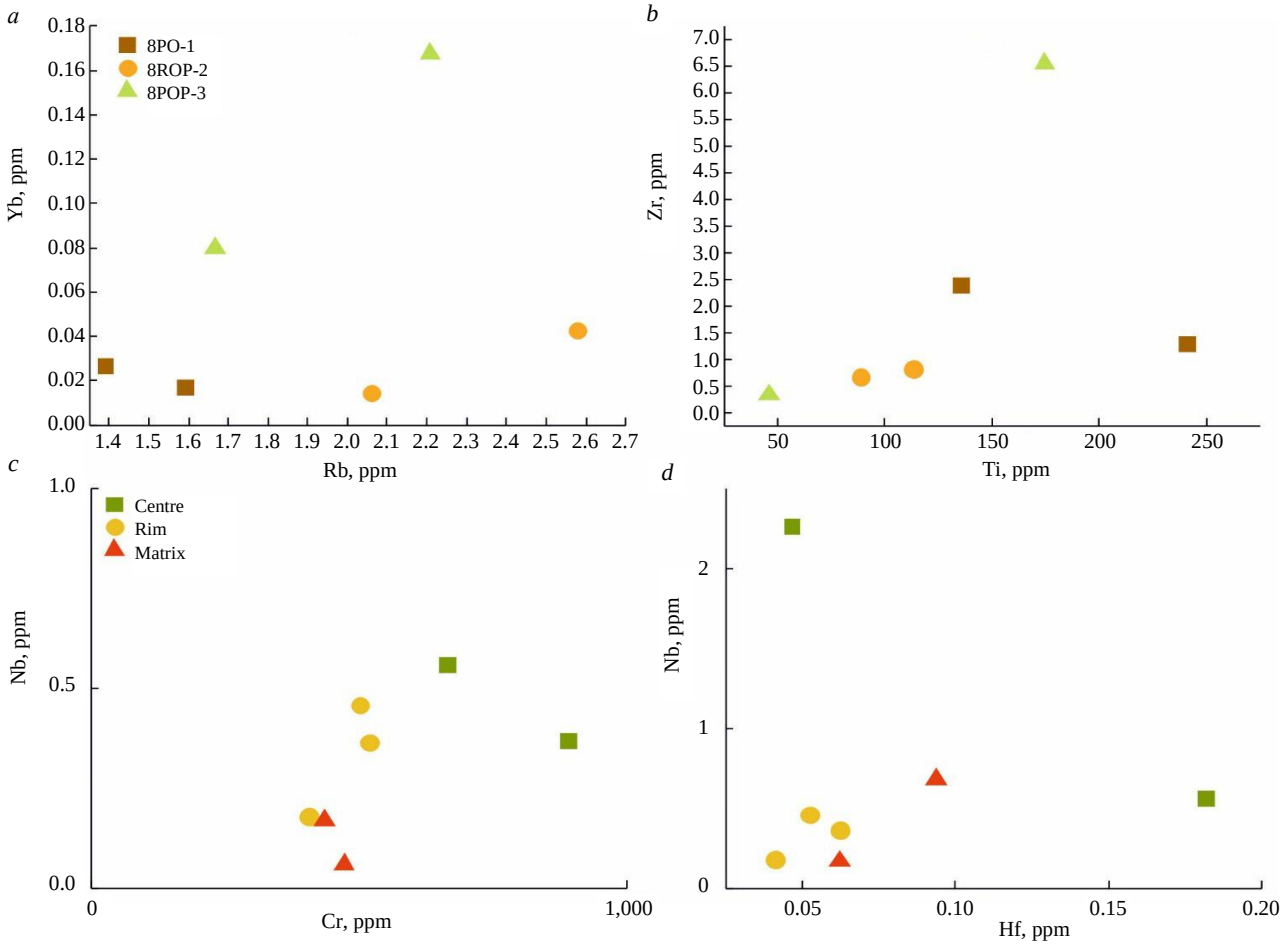



Fig.5. The Yb/Rb (*a*), Zr/Ti (b), Nb/Cr (*c*) and Nb/Hf (*d*) in olivine from Kunashak Meteorite

The diagram for refractory Zr-Ti relationship, conversely, shows that olivine in porphyritic olivine chondrule 8PO-1 is enriched in these elements, while olivine in the radiated chondrule is impoverished in them, and olivine in porphyritic chondrule 8POP-3 may show different values.

The diagram for Cr-Nb relationship (Fig.5, *в*) shows a difference between olivine in the centre of the chondrules enriched in these elements and olivine on the chondrule margin and in the matrix of the meteorite, which is usually impoverished in them.

The relationship of refractory Hf and Nb (Fig.5, *d*) also indicates elevated concentrations of the above elements in olivine in the centre of the chondrule and minimum concentrations in olivine on the chondrule margin and in the matrix of the meteorite.

Trace element distribution spectra in low-Ca pyroxene are more differentiated than spectra for olivine, indicating elevated trace element concentrations in pyroxene from porphyritic chondrules (8PO-1, 8POP-3) (see Fig.4, *c*). No considerable differences between low-Ca pyroxene in the centre and on the margin of the chondrule, as well as the meteorite matrix, were revealed, but pyroxene grains in the centre of the chondrule tend to be enriched in trace elements (see Fig.4, *d*).

Low-Ca pyroxene in radiated chondrule 8ROP-2 is clearly different, as shown by diagrams for Zr/Cr, Hf/Yb and Nb/Ti relationships (Fig.6, *a*, *c*, *e*). For instance, pyroxene in the radiated chondrule has higher Cr, Yb, Nb and Ti concentrations than pyroxenes in porphyritic chondrules, which display no differences.

The diagrams showing Nb-Hf, HREE-Rb and Zr-Yb relationships (Fig.6, *b*, *d*, *f*) indicate the enrichment of low-Ca pyroxene in the central zones of the chondrule relative to low-Ca pyroxene on the chondrule margin and in the meteorite matrix. The diagram for Nb and Hf shows that these elements are directly correlated in pyroxene from the chondrule margin and the meteorite matrix, which is not traced in pyroxene from the centre of the chondrule. HREE-Rb relationship indicates that its value tends to increase upon transition from pyroxene in the meteorite matrix to pyroxene on the chondrule margin. Low-Ca pyroxene in the centre of the chondrule has the highest HREE and Rb concentrations.


*This is an open access article under the CC BY 4.0 license*

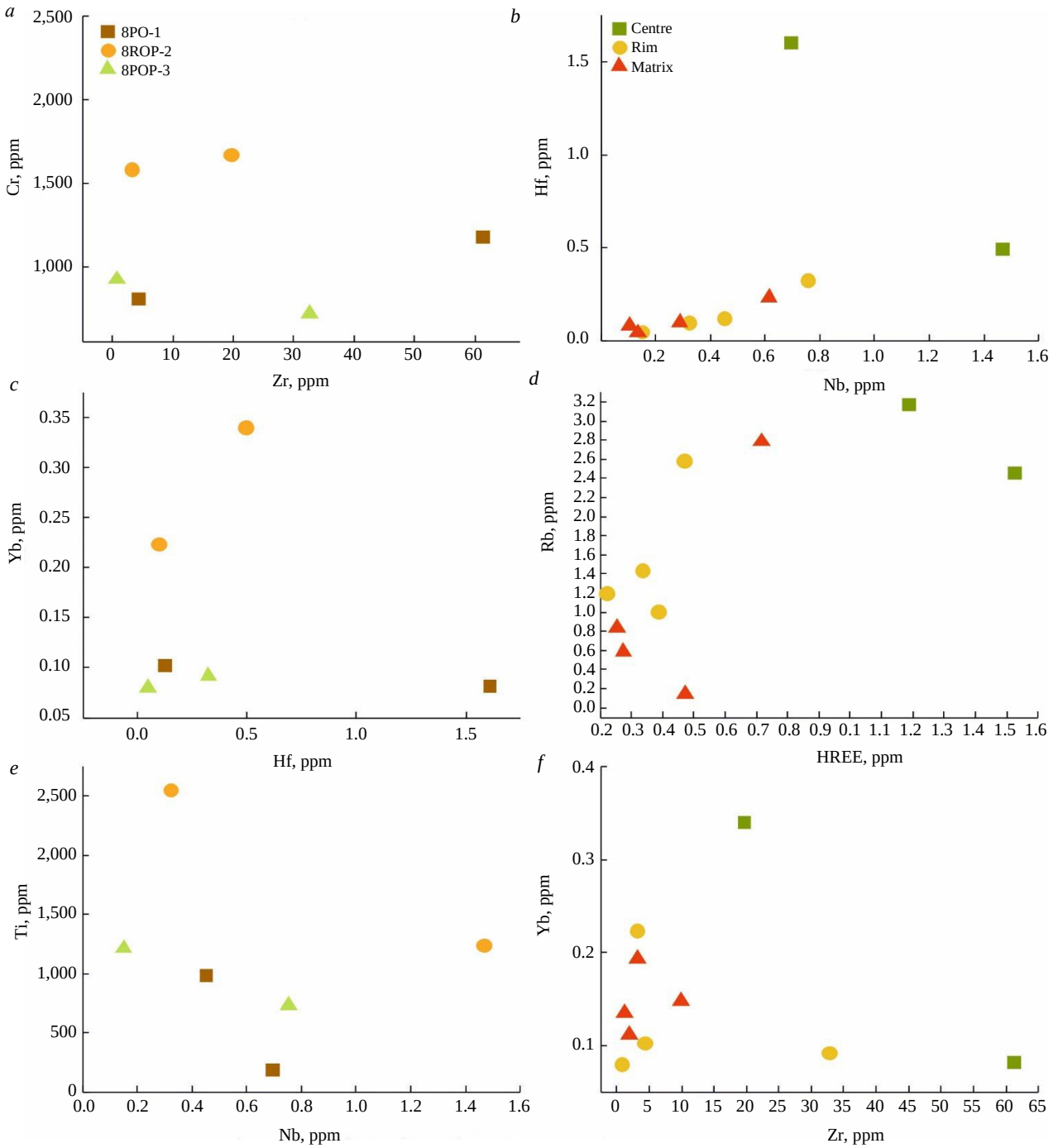



Fig.6. The Cr/Zr (*a*), Hf/Nb (*b*), Yb/Hf (*c*), Rb/HREE (*d*), Ti/Nb (*e*), Yb/Zr (*f*) ratios in low-Ca pyroxene from Kunashak Meteorite

Plagioclase displays the greatest differentiation of trace element distribution spectra in comparison with olivine and low-Ca pyroxene in Kunashak Meteorite (see Fig.4, *e*). Plagioclase from the chondrules analyzed is similar in trace element distribution spectra to plagioclase from Renazzo coaly chondrite. A similar spectrum was obtained for plagioclase from the most heavily metamorphosed ordinary chondrites. This evidence is supported by petrological type VI of Kunashak Meteorite.

Plagioclase in radiated chondrule 8ROP-2 is remarkable for its spectrum, which is most similar to plagioclase from Vigarano coaly chondrite and differs in elevated refractory and REE concentrations from other plagioclases in Kunashak Meteorite.

No significant differences between trace element distribution spectra in plagioclase from the centre, margin or matrix of the meteorite have been found, although plagioclase from the chondrule



*This is an open access article under the CC BY 4.0 license*

margin tends to be impoverished in trace elements, as compared with plagioclase from the central zone of the chondrule and the matrix of the meteorite (see Fig.4, *f*).

Differences between plagioclase in chondrules 8PO-1, 8POP-3 and 8ROP-2 are shown on diagrams for Sr-Ba, Ti-Y and Zr-Y relationships (Fig.7, *a*, *c*, *e*). The correlation of moderately volatile compatible Sr and Ba indicates that plagioclase from porphyritic chondrules is enriched in Ba and is poor in Sr, while plagioclase from the radiated chondrule displays a reverse distribution with high Sr and low Ba concentrations.

The graph of the Y and Ti ratio shows a direct correlation, in which the plagioclase of the porphyritic olivine chondrule is depleted in these elements, the plagioclase of the radial chondrule is enriched in them, and the plagioclase of the porphyritic olivine-pyroxene chondrule occupies an intermediate position.

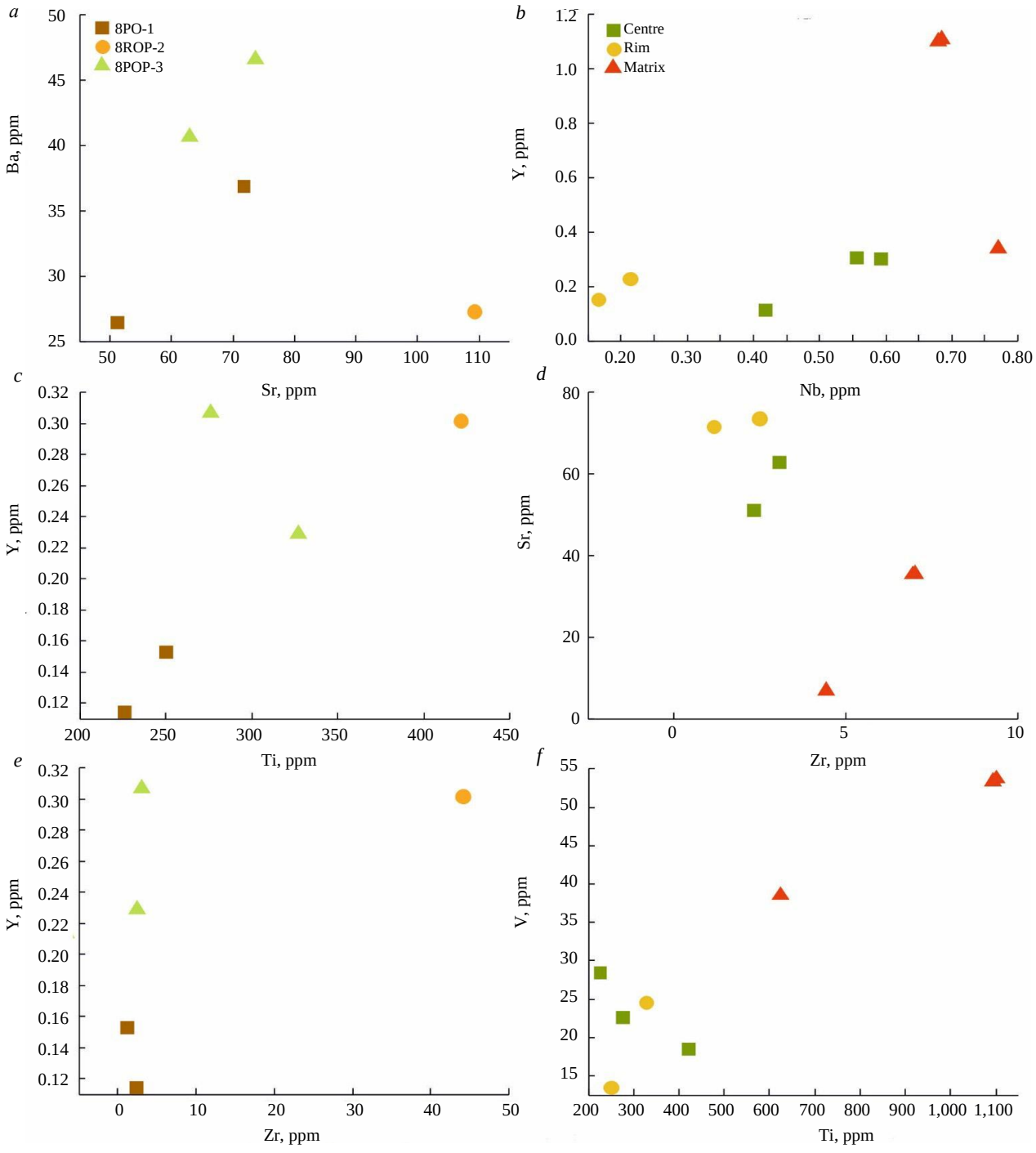



Fig.7. The Ba/Sr (*a*), Y/Nb (*b*), Y/Ti (*c*), Sr/Zr (*d*), Y/Zr (*e*), V/Ti (*f*) ratios in plagioclase from Kunashak Meteorite



*This is an open access article under the CC BY 4.0 license*

The Zr and Y ratio reflects the enrichment of the plagioclase of the porphyritic olivine-pyroxene chondrule in Y, high concentrations of Zr in the plagioclase of the radial chondrule and a low content of both elements in the plagioclase of the porphyritic olivine chondrule. The ratio of Nb/Y, Zr/Sr and Ti/V allows us to identify the characteristic features of the trace element composition of the plagioclase of the center, the rim of the chondrule and the matrix of the meteorite (Fig.7, *b*, *d*, *e*). The chondrules typically display low Sr and Ba concentrations. Plagioclase from the centre of the chondrules occupies an intermediate position with respect to Nb concentration.

The diagram for Zr and Sr shows a gradual decline in moderately volatile Sr concentration and a rise in Zr concentration from the margin to the centre of the chondrule and then to the meteorite matrix.

Also, plagioclase from the meteorite matrix has high refractory Ti and moderately volatile V concentrations, although plagioclase from the chondrules is typically poor in Ti and V.

**Conclusion.**

Porphyritic olivine-pyroxene chondrule 8POP-3 contains elevated trace element concentrations in olivine and especially the highest Yb concentrations (~0.12 ppm) in comparison with chondrules 8PO-1 and 8ROP-2 (0.02 ppm).

Radiated chondrule 8ROP-2 contains low-Ca pyroxene and plagioclase with high trace element concentrations. Low-Ca pyroxee typically has elevated Yb, Cr, Nb and Ti concentrations. Pyroxene from porphyritic chondrules contains minimum concentrations of the above elements. Plagioclase from the radiated chondrule is rich in Sr, Y, Ti, and Zr. Elevated trace element concentrations in low-Ca pyroxene and plagioclase from the radiated chondrule are indicative of rapid chondrule crystallization (over 1,000 °C/h). The incompatible LREE and Ba distribution coefficient in olivine and low-Ca pyroxene was found to increase 100-fold when cooling rate increases, but it becomes only twice as high for compatible Yb and Lu [41].

Thus, the trace element composition of silicate minerals from Kunashak Meteorite has retained the individual distinctive features of chondrule melting, and was not affected by thermal metamorphism on parent chondrite bodies. Similar results were obtained by studying Bushkhov Meteorite (L6) [34]. We are sure that trace elements in olivine and low-Ca pyroxene are resistant to thermal metamorphism.

The persistence of the distinctive features of chondrules enables us to use equilibrated ordinary chondrites for study of processes that took place at early stages in the formation of the Solar System and for a better understanding of chondrule and planet formation mechanisms.

*The authors are grateful to S.G.Simakin and E.V.Potapov (Valiev IPT, RAS, Yaroslavl Branch) for analytical work.*

**REFERENCES**

1. Krinov E.L. Kunashak stone meteor shower. *Meteoritika*. 1950. N 8, p. 66-77 (in Russian).
2. Yudin I.A. New data on the Kunashak meteorite shower. *Meteoritika*. 1951. N 9, p. 122-123 (in Russian).
3. Erokhin Y.V., Koroteev V.A., Khiller V.V. et al. Kunashak meteorite: new data on mineralogy. *Doklady Earth Sciences.* 2015. Vol. 464. N 2, p. 1058-1061. DOI: 10.1134/S1028334X15100128
4. Yudin I.A. On the presence of meteoric dust in the area of the fall of the Kunashak meteorite shower. *Meteoritika*. 1960. N 18, p. 113-118 (in Russian).
5. Zotkin I.T., Krinov E.L. Study of the conditions of the fall of the Kunashak meteorite shower. *Meteoritika*. 1958. N 15, p. 51-81 (in Russian).
6. Tsvetkov V. On meteorite orbits. *Earth, Moon, and Planets*. 1987. Vol. 37. Iss. 2, p. 133-140. DOI: 10.1007/BF00130888
7. Lindsay S.S., Dunn T.L., Emery J.P., Bowles N.E. The Red Edge Problem in asteroid band parameter analysis. *Meteoritics & Planetary Science*. 2016. Vol. 51. Iss. 4, p. 806-817. DOI: 10.1111/maps.12611
8. Pape J., Mezger K., Bouvier A.-S., Baumgartner L.P. Time and duration of chondrule formation: Constraints from $^{26}$Al-$^{26}$Mg ages of individual chondrules. *Geochimica et Cosmochimica Acta*. 2019. Vol. 244, p. 416-436. DOI: 10.1016/j.gca.2018.10.017
9. Piralla M., Villeneuve J., Batanova V. et al. Conditions of chondrule formation in ordinary chondrites. *Geochimica et Cosmochimica Acta*. 2021. Vol. 313, p. 295-312. DOI: 10.1016/j.gca.2021.08.007
10. Hewins R.H., Connolly H.C., Lofgren Jr. G.E., Libourel G. Experimental Constraints on Chondrule Formation. Chondrites and the protoplanetary disk: Proceedings of a workshop held at the Radisson Kaua'i Beach Resort, 8-11 November 2004, Kaua'i, Hawai'i. San Francisco: Astronomical Society of the Pacific, 2005. Vol. 341, p. 286-316.
11. Russell S.S., Connolly Jr. H.C., Krot A.N. Chondrules. Records of Protoplanetary Disk Processes. Cambridge University Press, 2018, p. 56. DOI: 10.1017/9781108284073
12. Jacquet E., Piralla M., Kersaho P., Marrocchi Y. Origin of isolated olivine grains in carbonaceous chondrites. *Meteoritics & Planetary Science*. 2021. Vol. 56. Iss. 1, p. 13-33. DOI: 10.1111/maps.13583



*This is an open access article under the CC BY 4.0 license*

13. Marrocchi Y., Euverte R., Villeneuve J. et al. Formation of CV chondrules by recycling of amoeboid olivine aggregate-like precursors. *Geochimica et Cosmochimica Acta*. 2019. Vol. 247, p. 121-141. DOI: 10.1016/j.gca.2018.12.038
14. Nardi L., Palomba E., Longobardo A. et al. Mapping olivine abundance on asteroid (25143) Itokawa from Hayabusa/NIRS data. *Icarus*. 2019. Vol. 321, p. 14-28. DOI: 10.1016/j.icarus.2018.10.035
15. Jacquet E., Marrocchi Y. Chondrule heritage and thermal histories from trace element and oxygen isotope analyses of chondrules and amoeboid olivine aggregates. *Meteoritics & Planetary Science*. 2017. Vol. 52. Iss. 12, p. 2672-2694. DOI: 10.1111/maps.12985
16. Libourel G., Krot A.N. Evidence for the presence of planetesimal material among the precursors of magnesian chondrules of nebular origin. *Earth and Planetary Science Letters*. 2007. Vol. 254. Iss. 1-2, p. 1-8. DOI: 10.1016/j.epsl.2006.11.013
17. Tenner T.J., Nakashima D., Ushikubo T. et al. Oxygen isotope ratios of FeO-poor chondrules in CR3 chondrites: Influence of dust enrichment and $H_2O$ during chondrule formation. *Geochimica et Cosmochimica Acta*. 2015. Vol. 148, p. 228-250. DOI: 10.1016/j.gca.2014.09.025
18. Varela M.E., Zinner E. Unraveling the role of liquids during chondrule formation processes. *Geochimica et Cosmochimica Acta*. 2018. Vol. 221, p. 358-378. DOI: 10.1016/j.gca.2017.03.038
19. Ruzicka A.M., Greenwood R.C., Armstrong K. et al. Petrology and oxygen isotopic composition of large igneous inclusions in ordinary chondrites: Early solar system igneous processes and oxygen reservoirs. *Geochimica et Cosmochimica Acta*. 2019. Vol. 266, p. 497-528. DOI: 10.1016/j.gca.2019.01.017
20. Bischoff A., Schleiting M., Wieler R., Patzek M. Brecciation among 2280 ordinary chondrites – Constraints on the evolution of their parent bodies. *Geochimica et Cosmochimica Acta*. 2018. Vol. 238, p. 516-541. DOI: 10.1016/j.gca.2018.07.020
21. Lewis J.A., Jones R.H., Garcea S.C. Chondrule porosity in the L4 chondrite Saratov: Dissolution, chemical transport, and fluid flow. *Geochimica et Cosmochimica Acta*. 2018. Vol. 240, p. 293-313. DOI: 10.1016/j.gca.2018.08.002
22. Varela M.E. Bulk trace elements of Mg-rich cryptocrystalline and ferrous radiating pyroxene chondrules from Acfer 182: Their evolution paths. *Geochimica et Cosmochimica Acta*. 2019. Vol. 257, p. 1-15. DOI: 10.1016/j.gca.2019.04.025
23. Levashova E.V., Mamykina M.E., Skublov S.G. et al. Geochemistry (TE, REE, Oxygen) of Zircon from Leucogranites of the Belokurikhinsky Massif, Gorny Altai, as Indicator of Formation Conditions. *Geochemistry International*. 2023. Vol. 61. Iss. 13, p. 1323-1339. DOI: 10.1134/S001670292311006X
24. Skublov S.G., Rumyantseva N.A., Vanshtein B.G. et al. Zircon Xenocrysts from the Shaka Ridge Record Ancient Continental Crust: New U-Pb Geochronological and Oxygen Isotopic Data. *Journal of Earth Science*. 2022. Vol. 33. Iss. 1, p. 5-16. DOI: 10.1007/s12583-021-1422-2
25. Skublov S.G., Levashova E.V., Mamykina M.E. et al. The polyphase Belokurikhinsky granite massif, Gorny Altai: isotope-geochemical study of zircon. *Journal of Mining Institute*. 2024, p. 24 (Online first).
26. Salimgaraeva L.I., Berezin A.V. Garnetites from Marun-Keu eclogite complex (Polar Urals): geochemistry and the problem of genesis. *Journal of Mining Institute*. 2023. Vol. 262, p. 509-525.
27. Stativko V.S., Skublov S.G., Smolenskiy V.V., Kuznetsov A.B. Trace and rare-earth elements in garnets from silicate-carbonate formations of the Kusa-Kopan complex (Southern Urals). *Lithosphere*. 2023. Vol. 23. N 2, p. 225-246 (in Russian). DOI: 10.24930/1681-9004-2023-23-2-225-246
28. Skublov S.G., Gavrilchik A.K., Berezin A.V. Geochemistry of beryl varieties: comparative analysis and visualization of analytical data by principal component analysis (PCA) and t-distributed stochastic neighbor embedding (t-SNE). *Journal of Mining Institute*. Vol. 255, p. 455-469. DOI: 10.31897/PMI.2022.40
29. Gavrilchik A.K., Skublov S.G., Kotova E.L. Trace Element Composition of Beryl from the Sherlovaya Gora Deposit, Southea-stern Transbaikal Region, Russia. *Geology of Ore Deposits*. 2022. Vol. 64. N 7, p. 442-451. DOI: 10.1134/s1075701522070054
30. Lichtenberg T., Golabek G.J., Dullemond C.P. et al. Impact splash chondrule formation during planetesimal recycling. *Icarus*. 2018. Vol. 302, p. 27-43. DOI: 10.1016/j.icarus.2017.11.004
31. Chakraborty S. Diffusion Coefficients in Olivine, Wadsleyite and Ringwoodite. *Reviews in Mineralogy and Geochemistry*. 2010. Vol. 72. N 1, p. 603-639. DOI: 10.2138/rmg.2010.72.13
32. Cherniak D.J. REE diffusion in olivine. *American Mineralogist*. 2010. Vol. 95. Iss. 2-3, p. 362-368. DOI: 10.2138/am.2010.3345
33. Marrocchi Y., Villeneuve J., Batanova V. et al. Oxygen isotopic diversity of chondrule precursors and the nebular origin of chondrules. *Earth and Planetary Science Letters*. 2018. Vol. 496, p. 132-141. DOI: 10.1016/j.epsl.2018.05.042
34. Sukhanova K.G., Skublov S.G., Galankina O.L. et al. Trace Element Composition of Silicate Minerals in the Chondrules and Matrix of the Buschhof Meteorite. *Geochemistry International*. 2020. Vol. 58. N 12, p. 1321-1330. DOI: 10.1134/S001670292012006X
35. Sukhanova K.G. Composition of silicate minerals as a reflection of the evolution of equilibrium ordinary chondrites: Avtoref. dis. … kand. geol.-mineral. nauk. Moscow: Moskovskii gosudarstvennyi universitet imeni M.V.Lomonosova, 2022, p. 21.
36. Batanova V.G., Suhr G., Sobolev A.V. Origin of Geochemical Heterogeneity in the Mantle Peridotites from the Bay of Islands Ophiolite, Newfoundland, Canada: Ion Probe Study of Clinopyroxenes. *Geochimica et Cosmochimica Acta*. 1998. Vol. 62. Iss. 5, p. 853-866. DOI: 10.1016/S0016-7037(97)00384-0
37. Portnyagin M., Almeev R., Matveev S., Holtz F. Experimental evidence for rapid water exchange between melt inclusions in olivine and host magma. *Earth and Planetary Science Letters*. 2008. Vol. 272. Iss. 3-4, p. 541-552. DOI: 10.1016/j.epsl.2008.05.020
38. Palme H., Lodders K., Jones A. 2.2 – Solar System Abundances of the Elements. Treatise on Geochemistry. Elsevier, 2014. Vol. 2: Planets, Asteriods, Comets and The Solar System, p. 15-36. DOI: 10.1016/b978-0-08-095975-7.00118-2
39. Jacquet E., Alard O., Gounelle M. Trace element geochemistry of ordinary chondrite chondrules: The type I/type II chondrule dichotomy. *Geochimica et Cosmochimica Acta*. 2015. Vol. 155, p. 47-67. DOI: 10.1016/j.gca.2015.02.005
40. Jacquet E., Alard O., Gounelle M. Chondrule trace element geochemistry at the mineral scale. *Meteoritics and Planetary Science*. 2012. Vol. 47. Iss. 11, p. 1695-1714. DOI: 10.1111/maps.12005
41. Kennedy A.K., Lofgren G.E., Wasserburg G.J. An experimental study of trace element partitioning between olivine, orthopyroxene and melt in chondrules: equilibrium values and kinetic effects. *Earth and Planetary Science Letters*. 1993. Vol. 115. Iss. 1-4, p. 177-195. DOI: 10.1016/0012-821X(93)90221-T

***Authors:*** **Kristina G. Sukhanova,** *Candidate of Geological and Mineralogical Sciences, Junior Researcher, cris.suhanova92@yandex.ru, https://orcid.org/0000-0001-5695-0767* (*Institute of Precambrian Geology and Geochronology RAS, Saint Petersburg, Russia*), **Olga L. Galankina,** *Candidate of Geological and Mineralogical Sciences, Senior Researcher, https://orcid.org/0000-0003-2761-2835* (*Institute of Precambrian Geology and Geochronology RAS, Saint Petersburg, Russia*).

*The authors declare no conflict of interests.*



*This is an open access article under the CC BY 4.0 license*